

Endowing Language Models with Multimodal Knowledge Graph Representations

Ningyuan (Teresa) Huang¹ Yash R. Deshpande² Yibo Liu² Houda Alberts^{3,*}
Kyunghyun Cho² Clara Vania^{4,†} Iacer Calixto^{2,5}

¹Johns Hopkins University, USA ²New York University, USA

³Rond Consulting, NL ⁴Amazon Alexa AI, UK

⁵Amsterdam UMC, University of Amsterdam, Dept. of Medical Informatics, Amsterdam, NL
{nh1724, yd1282, yl6769, ic1179}@nyu.edu

Abstract

We propose a method to make natural language understanding models more parameter efficient by storing knowledge in an external knowledge graph (KG) and retrieving from this KG using a dense index. Given (possibly multilingual) downstream task data, e.g., sentences in German, we retrieve entities from the KG and use their multimodal representations to improve downstream task performance. We use the recently released VisualSem KG as our external knowledge repository, which covers a subset of Wikipedia and WordNet entities, and compare a mix of tuple-based and graph-based algorithms to learn entity and relation representations that are grounded on the KG multimodal information. We demonstrate the usefulness of the learned entity representations on two downstream tasks, and show improved performance on the multilingual named entity recognition task by 0.3%–0.7% F1, while we achieve up to 2.5% improvement in accuracy on the visual sense disambiguation task.¹

1 Introduction

Recent natural language understanding (NLU) and generation (NLG) models obtain increasingly better state-of-the-art performance across benchmarks (Wang et al., 2019b,a; Hu et al., 2020), however at the cost of a daunting increase in number of model parameters (Radford et al., 2019; Brown et al., 2020; Fedus et al., 2021).² These increasingly large models lead to ever-increasing financial, computational, and environmental costs (Strubell et al., 2019). To make large language models (LMs) more parameter efficient, existing approaches propose to distill a compressed model given a large

LM (Sanh et al., 2019) or to promote parameter sharing directly in the large LM (Lan et al., 2020).

In this work, we advocate for an orthogonal approach: to augment language models by retrieving multimodal representations from external structured knowledge repositories. In this way, LMs themselves need not store all this knowledge implicitly in their parameters (Petroni et al., 2019; Nematzadeh et al., 2020). Concretely, we investigate different methods to learn representations for entities and relations in the VisualSem (VS; Alberts et al., 2021) structured knowledge graph (KG). We demonstrate the usefulness of the learned KG representations in multilingual named entity recognition (NER) and crosslingual visual verb sense disambiguation (VSD). In particular, we use the VS KG since it is a publicly available multilingual and multimodal KG designed to support vision and language research, and it provides a multimodal retrieval mechanism that allows neural models to retrieve entities from the KG using arbitrary queries. In order to ground the downstream NER and VSD tasks with structured knowledge, we use VisualSem’s *sentence retrieval* model to map input sentences into entities in the KG, and use the learned entity representations as features.

We investigate different methods to learn representations for entities and relations in VS, including tuple-based and graph-based neural algorithms. We incorporate VS textual descriptions in 14 diverse languages as well as multiple images available for each entity in our representation learning framework. Entity and relation representations are trained to be predictive of the knowledge graph structure, and we share them publicly with the research community to encourage future research in this area. We illustrate our framework in Figure 1. Our main contributions are:

Our main contributions are:

- We compare the performance of different tuple- and graph-based representation learning algorithms for the VisualSem KG.

*Work done while at the University of Amsterdam.

†Work done while at New York University.

¹All our code and data are available in: <https://github.com/iacercalixto/visualsem-kg>.

²Although the OpenAI GPT-2, OpenAI GPT-3, and Google Switch models were released within a 2-years time span, they boast 1.5B, 175B, and 1.6T parameters, respectively.

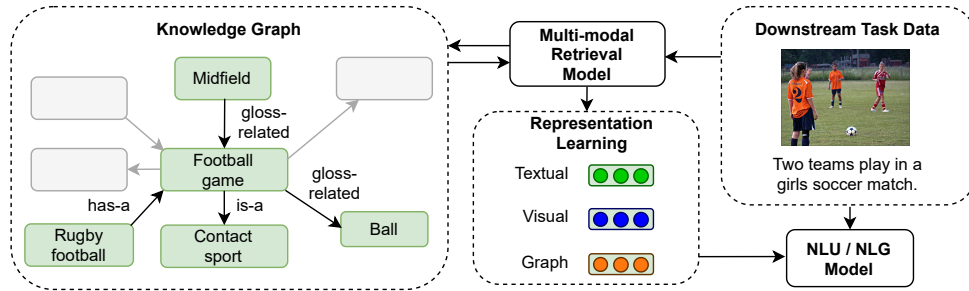


Figure 1: We learn visual, textual, and structural representations for a knowledge graph (KG). We propose to use this KG as an external knowledge repository, which we query using *downstream task* sentences. We use the retrieved entities’ representations to ground inputs in named entity recognition and visual verb sense disambiguation.

- We demonstrate the usefulness of the learned representations on multilingual NER and crosslingual VSD, where we find that incorporating relevant retrieved entity representations improves model performance by up to 0.7% F1 on NER and by up to 2.5% accuracy in VSD.
- We publicly release our learned representations for entities and relations to encourage future research in this area.

This paper is organised as follows. In Section 2 we discuss relevant related work, including solutions to endow models with access to external knowledge. In Section 3 we briefly discuss VisualSem as well as notation we use throughout the paper. In Section 4 we introduce the representation learning methods used in our experiments. In Sections 5, 6 and 7, we introduce our experimental setup, evaluate and compare the learned representations with different architectures, and investigate the impact different modalities (i.e. textual and visual) have on the learned representations, respectively. In Section 8, we report experiments using the learned representations on downstream tasks. Finally, in Section 9 we discuss our main findings as well as provide avenues for future work.

2 Related work

Memory in Neural Models Endowing models with an external memory is not a new endeavour (Das et al., 1992; Zheng Zeng et al., 1994). Approaches more directly relevant to our work include memory networks (Weston et al., 2014; Sukhbaatar et al., 2015) and neural Turing machines (Graves et al., 2014), both proposed as learning frameworks that endow neural networks with an external memory that can be read from and written to.

Related to our *multimodal* setting, Xiong et al. (2016) proposed memory networks for textual question answering (QA) and visual QA, where the memory module attends to the relevant visual features given the textual representations. To address the issue where questions cannot be directly answered by the given visual content, Su et al. (2018) proposed visual knowledge memory networks that produce joint embedding of KG triplets and visual features. Wang et al. (2018) also applied a multi-modal memory model (M^3) to the video captioning task. In all cases, memories are trained using task data and are used as a kind of *working memory* (Nematzadeh et al., 2020).

Retrieval augmented models In retrieval augmented models, memories are initialized with external knowledge beyond the data available for the task. Lee et al. (2019) proposed a framework for Open Retrieval QA (ORQA) where the retrieval and QA modules are jointly trained. Karpukhin et al. (2020) learned a dense passage retriever (DPR) and improved retrieval quality compared to standard sparse retrieval mechanisms, e.g., TF-IDF or BM25, which led to improvements on QA when using retrieved facts. REALM (Gua et al., 2020) uses a dense Wikipedia index and fine-tunes the index together with a pretrained language model to address open-domain QA tasks. Petroni et al. (2020) studied how feeding BERT with contexts retrieved/generated in different ways affects its performance on unsupervised QA without external knowledge. Finally, Lewis et al. (2020) proposed a retrieval augmented generation model where an encoder-decoder model learns to generate answers to questions conditioned on Wikipedia.

However, most existing retrieval augmented models based on Wikipedia do not usually include visual information or use the structure in the KG.

In this work, we propose a framework to retrieve multimodal information that encodes the structural information in the KG.

Multimodal pretraining Recently, pretrained vision and language models have achieved state-of-the-art results across many multimodal reasoning tasks (Tan and Bansal, 2019; Lu et al., 2019; Yu et al., 2021). This line of work explicitly learns connections between vision and language inputs based on masked multimodal modelling over image-text pairs. By contrast, we focus on modelling entities and relations in an *entity-centric structured KG*, i.e., a KG where nodes denote concepts and contain multimodal information.

3 VisualSem Knowledge Graph

VisualSem (Alberts et al., 2021) is a multilingual and multimodal KG consisting of over 100k nodes, 1.9 million relations between nodes, and 1.5 million associated images, built using BabelNet v4.0 (Navigli and Ponzetto, 2012) and ImageNet (Rusakovskiy et al., 2015). Each node denotes a *synset* and is illustrated by multiple images.³ VS covers many diverse topics and has 13 relation types with a strong visual component: *is-a*, *has-part*, *related-to*, *used-for*, *used-by*, *subject-of*, *receives-action*, *made-of*, *has-property*, *gloss-related*, *synonym*, *part-of*, and *located-at*. See Alberts et al. (2021) for more details about the KG.

To the best of our knowledge, VS is the only publicly available multimodal KG designed to be integrated into neural model pipelines, and thus chosen in our experiments. Nonetheless, our framework can be applied to any KG.

Notation Let the KG be a directed graph $\mathcal{G} = (\mathcal{V}, \mathcal{E})$, where \mathcal{V} is the set of vertices or nodes, i.e., the KG *synsets*, and \mathcal{E} is the set of edges consisting of *typed relations* between two synsets. We refer to nodes v_j connected to v_i by any relation as part of v_i 's local neighborhood \mathcal{N}_i , i.e., $\forall v_j \in \mathcal{N}_i, v_j$ is related to v_i by some relation e_r in \mathcal{E} .

Let \mathcal{D} be the set of all tuples (v_i, e_r, v_j) in the KG, i.e., all tuples where a *head* node $v_i \in \mathcal{V}$ is related to a *tail* node $v_j \in \mathcal{V}$ via a typed relation $e_r \in \mathcal{E}$ with *type* r . Let \mathcal{D}' be the set of corrupted tuples (v_i, e_r, v'_j) , where (v_i, e_r, v'_j) is not in \mathcal{G} , and the tail node v'_j (or head node v'_i) is randomly cor-

³A synset is a concept and can be described in many languages, e.g., synset *dog* has associated description *The dog is a mammal in the order Carnivora*.

rupted and not related to v_i (or v_j) via e_r . We learn representations for \mathcal{G} including a node embedding matrix $\mathbf{V} \in \mathbb{R}^{|\mathcal{V}| \times d_n}$ and an edge embedding matrix $\mathbf{E} \in \mathbb{R}^{|\mathcal{E}| \times d_r}$, where d_n, d_r are node and relation embedding dimensions, respectively. Node v_i 's embedding \mathbf{v}_i is the column vector $\mathbf{V}[i, :]$, and relation e_r 's embedding \mathbf{e}_r is the column vector $\mathbf{E}[r, :]$. Each node $v_i \in \mathcal{V}$ is also associated to a set of *multilingual glosses* \mathcal{T}_i and *images* \mathcal{I}_i . Finally, we denote $[\mathbf{x}; \mathbf{y}]$ as the concatenation of \mathbf{x} and \mathbf{y} , and $\mathbf{x} \odot \mathbf{y}$ as the element-wise multiplication.

4 Knowledge Representation Learning

We are interested in learning robust multimodal representations for \mathcal{V} and \mathcal{E} that are useful in a wide range of downstream tasks. Next, we explore various tuple- and graph-based algorithms proposed to learn structured knowledge representations.

4.1 Tuple-based algorithms

Most tuple-based algorithms represent knowledge as a factual triple in the form of (*head, relation, tail*) or using our previous notation, (v_i, e_r, v_j) , with its respective embeddings $(\mathbf{v}_i, \mathbf{e}_r, \mathbf{v}_j)$.

TransE TransE (Bordes et al., 2013) is a seminal neural KB embedding model. It represents relations as translations in embedding space, where the embedding of the tail \mathbf{v}_j is trained to be close to the embedding of the head \mathbf{v}_i plus the relation vector \mathbf{e}_r , i.e., $\mathbf{v}_i + \mathbf{e}_r - \mathbf{v}_j \approx \mathbf{0}$.

DistMult The DistMult algorithm (Yang et al., 2015) is similar to TransE but uses a weighted element-wise dot product (*multiplicative* operation) to combine two entity vectors. The score for a triplet (v_i, e_r, v_j) is computed as

$$\phi(v_i, e_r, v_j) = \mathbf{v}_i \odot \mathbf{e}_r \odot \mathbf{v}_j. \quad (1)$$

TuckerER TuckerER (Balazevic et al., 2019) models a KG as a three-dimensional tensor $\mathcal{X} \in \mathbb{R}^{|\mathcal{V}| \times |\mathcal{E}| \times |\mathcal{V}|}$, and uses a Tucker decomposition (Tucker, 1966) to decompose $\mathcal{X} \approx \mathcal{W} \times_1 \mathbf{V} \times_2 \mathbf{E} \times_3 \mathbf{V}$, with \times_n indicating the tensor product along the n -th mode, and \mathcal{W} is the core tensor.

The score function of a tuple is defined as $\phi(v_i, e_r, v_j) = \mathcal{W} \times_1 \mathbf{v}_i \times_2 \mathbf{e}_r \times_3 \mathbf{v}_j$. Unlike TransE and DistMult which encode each tuple information directly into the relevant node (\mathbf{V}) and relation (\mathbf{E}) embeddings, TuckerER stores shared information across different tuples in \mathcal{W} .

4.2 Graph-based algorithms

Graph-based models compute node (and optionally edge) representations by learning an *aggregation function* over node embeddings connected by its relations in the graph (Battaglia et al., 2018).

GraphSage The GraphSage (Hamilton et al., 2017) algorithm computes node hidden states \mathbf{h}_i by subsampling and aggregating node v_i 's (subsampled) neighbors' states $\mathbf{h}_j, \forall v_j \in \mathcal{N}_i$. We use GraphSage without subsampling and choose mean aggregation function, where the l -th layer hidden states are computed as:

$$\mathbf{h}_i^{(l+1)} = \text{ReLU} \left(\sum_{v_j \in \mathcal{N}_i} \frac{1}{|\mathcal{N}_i|} \mathbf{W}_s^{(l)} \mathbf{h}_j^{(l)} \right) \quad (2)$$

where $\mathbf{W}_s^{(l)}$ is a trained weight matrix. In the first layer, $\mathbf{h}_j^{(l)}$ are set to the node embeddings v_j . This is also similar to the formulation in graph convolutional networks (GCNs; (Kipf and Welling, 2016)).

GAT In graph attention networks (GAT; Veličković et al., 2018), node hidden states $\mathbf{h}_i^{(l+1)}$ are computed by aggregating neighboring nodes $\mathbf{h}_j, \forall v_j \in \mathcal{N}_i$, using an attention mechanism.

$$\mathbf{h}_i^{(l+1)} = \sigma \left(\sum_{j \in \mathcal{N}_i} \alpha_{ij}^{(l)} \mathbf{z}_j^{(l)} \right), \quad (3)$$

$$\mathbf{z}_i^{(l)} = \mathbf{W}_g^{(l)} \mathbf{h}_i^{(l)}, \quad (4)$$

where $\mathbf{W}_g^{(l)}$ is a matrix used to linearly project nodes states $\mathbf{h}_i^{(l)}$ and σ is the sigmoid non-linearity. $\alpha_{ij}^{(l)}$ are attention scalar weights, computed as:

$$\alpha_{ij}^{(l)} = \frac{\exp \left(\gamma \left([\mathbf{z}_i^{(l)}; \mathbf{z}_j^{(l)}] \cdot \mathbf{a}^{(l)} \right) \right)}{\sum_{k \in \mathcal{N}_i} \exp \left(\gamma \left([\mathbf{z}_i^{(l)}; \mathbf{z}_k^{(l)}] \cdot \mathbf{a}^{(l)} \right) \right)}, \quad (5)$$

where $\mathbf{a}^{(l)}$ is a trained vector used to combine pairs of hidden states, and γ is the LeakyReLU non-linearity. The overall mechanism is based on the additive attention mechanism introduced in Bahdanau et al. (2015).

For simplicity, throughout the paper we denote the output of the last graph layer (GraphSage or GAT) for nodes $v_i \in \mathcal{V}$ to be \mathbf{h}_i (without the layer superscript).

4.2.1 Hybrid models

We also experiment with hybrid models where we combine a graph-based model with a DistMult layer for prediction, since GraphSage and GAT do not normally use relation information in their message passing algorithms. We are inspired by relational graph convolutional networks (Schlichtkrull et al., 2017) where a DistMult layer was added to graph convolutional networks. For a triplet (v_i, e_r, v_j) , given hidden states \mathbf{h}_i and \mathbf{h}_j generated from a graph-based model (GraphSage or GAT), we compute the triplet score in Equation 1 by replacing v_i, v_j with $\mathbf{h}_i, \mathbf{h}_j$, respectively.

4.3 Multimodal Node Features

Each node $v_i \in \mathcal{V}$ includes two sets of additional features: textual features \mathbf{t}_i for glosses \mathcal{T}_i , and visual features \mathbf{m}_i for images \mathcal{I}_i .

Gloss Features Let $t_{i,g}$ be the g -th gloss in \mathcal{T}_i . We extract features $\mathbf{t}_{i,g}$ for each gloss $t_{i,g} \in \mathcal{T}_i$ using Language-Agnostic Sentence Representations (LASER; Artetxe and Schwenk, 2019), a 5-layer bidirectional LSTM model. LASER supports 93 languages and obtains strong performance on cross-lingual tasks such as entailment and document classification. We tokenize glosses using the LASER tokenizer for the respective language. Each gloss embedding $\mathbf{t}_{i,g} \in \mathcal{T}_i$ is a 1024-dimensional feature vector of max-pooled representations of the hidden states of the last bidirectional LSTM layer.

We aggregate text features \mathbf{t}_i for each node $v_i \in \mathcal{V}$ as the average of its gloss features.

$$\mathbf{t}_i = \frac{1}{|\mathcal{T}_i|} \sum_{g=1}^{|\mathcal{T}_i|} \mathbf{t}_{i,g}, \quad \forall t_{i,g} \in \mathcal{T}_i. \quad (6)$$

Images Features Let $m_{i,l}$ be the l -th image in \mathcal{I}_i . We extract features $\mathbf{m}_{i,l}$ for each image $m_{i,l} \in \mathcal{I}_i$ using a ResNet-152 (He et al., 2016) architecture pretrained on ImageNet classification (Rusakovsky et al., 2015). We set each image embedding $\mathbf{m}_{i,l}$ to be the 2048-dimensional activation of the *pool5* layer.

Similarly as we do for glosses, we aggregate visual features \mathbf{m}_i for each node $v_i \in \mathcal{V}$ as the average of its image features.

$$\mathbf{m}_i = \frac{1}{|\mathcal{I}_i|} \sum_{l=1}^{|\mathcal{I}_i|} \mathbf{m}_{i,l}, \quad \forall m_{i,l} \in \mathcal{I}_i. \quad (7)$$

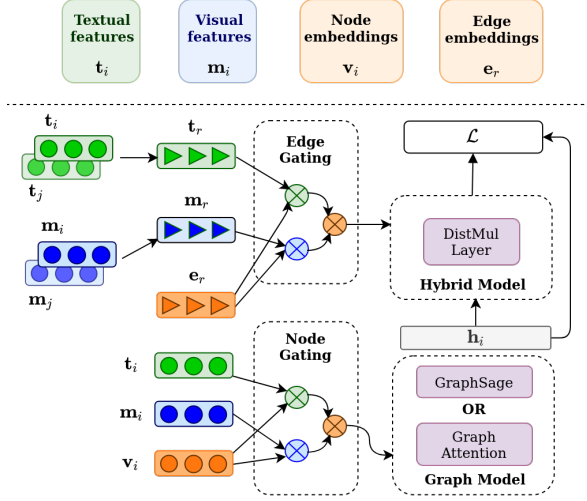


Figure 2: General architecture of our graph-based link prediction models. Node and edge embeddings \mathbf{V} and \mathbf{E} are trained and models optionally use textual and visual features t_i, m_i for node v_i to learn node and edge representations. Features are incorporated into node embeddings via node gating and into edge embeddings via edge gating, respectively.

4.3.1 Gating Text and Image Features

We gate gloss and image features $\{t_i, m_i\}$ in two different points in the model architecture: the node embeddings v_i , before feeding it into graph layers (GraphSage or GAT), henceforth *node gating*; and the edge hidden states e_r , before feeding it to the DistMult layer, henceforth *edge gating*. Figure 2 illustrates the node and edge gating mechanisms.

Node Gating We denote the node gating function f_n with trained parameters θ_n to transform node embeddings and additional features and compute *informed* node embeddings. For a given node embedding v_i , we can integrate: **1)** only textual features, in which case we have informed node embeddings $v_i^t = f_n(v_i, t_i; \theta_n)$; **2)** only image features, with informed node embeddings $v_i^m = f_n(v_i, m_i; \theta_n)$; or **3)** both textual and image features, with informed node embeddings $v_i^{t,m} = f_n(v_i, t_i, m_i; \theta_n)$. Please see Appendix C.1 for details on the architectures we use to compute f_n for (1), (2), and (3).

Edge (Relation) Gating Similarly to node gating, we denote the edge gating function f_e with parameters θ_e to transform edge embeddings and additional features and compute *informed* edge embeddings. For a given edge embedding e_r denoting an edge between nodes v_i and v_j , we integrate: **1)** only textual features, in which case we have informed

edge embeddings $e_r^t = f_e(v_i, t_i, v_j, t_j; \theta_e)$; **2)** only image features, with informed edge embeddings $e_r^m = f_e(v_i, m_i, v_j, m_j; \theta_e)$; or **3)** both textual and image features, with informed edge embeddings $e_r^{t,m} = f_e(v_i, t_i, m_i, v_j, t_j, m_j; \theta_e)$. Please see Appendix C.2 for details on the architectures we use to compute f_e for (1), (2), and (3).

5 Experimental Setup

We evaluate all models on the link prediction task, i.e., to identify whether there exists a *relation* between a pair of *head* and *tail* nodes. For each triplet (v_i, e_r, v_j) in the dataset, we create k corrupted triplets where the tail v_j (or the head v_i) is substituted by another node in the knowledge graph that is not connected with v_i (or v_j) under relation e_r . We experiment with $k = \{100, 1000\}$ corrupted examples per positive triplet. See Appendix C.3 for details on hybrid models GAT+DistMult and GraphSage+DistMult’s architectures.

Training All models are trained using negative sampling (Mikolov et al., 2013) to maximize the probability of positive triplets while minimizing the probability of k corrupted triplets.

$$\mathcal{L} = \frac{1}{|\mathcal{D}|} \sum_{(v_i, e_r, v_j) \in \mathcal{D}} \left[-\log \sigma(\phi(v_i, e_r, v_j)) - \sum_{(v_i, e_r, v'_j) \in \mathcal{D}'} \log \sigma(-\phi(v_i, e_r, v'_j)) \right], \quad (8)$$

where $\sigma(x)$ is the sigmoid function, \mathcal{D} is the set of triplets in the knowledge graph $(v_i, e_r, v_j) \in \mathcal{G}$, \mathcal{D}' is the set of corrupted triplets $(v_i, e_r, v'_j) \notin \mathcal{G}$.⁴

Scoring Function Let $\phi(v_i, e_r, v_j)$ be the scoring function of a triplet. For graph-based models, we compute the function as $\phi(v_i, e_r, v_j) = \mathbf{h}_i^\top \mathbf{h}_j$, i.e., there are no trained relation parameters. For hybrid models, we compute $\phi(v_i, e_r, v_j) = \mathbf{h}_i \odot e_r \odot \mathbf{h}_j$, i.e., we train the relation matrix \mathbf{E} .

When using multimodal features we replace the node embeddings input v_i with v_i^t when using text features, v_i^m when using image features, or $v_i^{t,m}$ when using both. For the hybrid models, in addition to the modified input, we also modify the input to the DistMult layer: instead of feeding e_r , we use e_r^t for the text features, e_r^m for the image features, or $e_r^{t,m}$ for both features.

⁴For TransE and DistMult, we use both head-corrupted (v'_i, e_r, v_j) and tail-corrupted triplets (v_i, e_r, v'_j)

| | MRR | Hits@1 | Hits@3 | Hits@10 |
|----------|------------|------------|------------|-------------|
| TransE | 3.2 | 0.2 | 3.3 | 8.2 |
| DistMult | 3.6 | 1.9 | 3.5 | 7.6 |
| Tucker | 6.1 | 3.4 | 6.3 | 11.1 |

Table 1: Link prediction results on VisualSem’s test set using all negative samples.

| | R | MRR | Hits@1 | Hits@3 | Hits@10 |
|-----------|---|-------------|-------------|--------------|--------------|
| TuckER | ✓ | 19.0 | 12.3 | 17.7 | 30.0 |
| GAT | ✗ | 10.0 | 3.8 | 12.6 | 29.7 |
| +DistMult | ✓ | 34.8 | 13.6 | 54.4 | 69.3 |
| GraphSage | ✗ | 8.6 | 2.3 | 6.4 | 18.0 |
| +DistMult | ✓ | 78.4 | 56.8 | 100.0 | 100.0 |

Table 2: Link prediction results on VisualSem’s test set using 100 negative samples. **R**: denotes whether the model learn relation features or not.

Evaluation We follow the standard evaluation for link prediction using the mean reciprocal rank (MRR), i.e., the mean of the reciprocal rank of the correct triplet, and Hits@{1, 3, 10}, i.e., the proportion of correct triplets ranked in the top-1, top-3 or top-10 retrieved entries, respectively. The higher the number of corrupted tuples k per positive example, the harder the task according to these metrics. Finally, all results are an average over 5 different runs, and in each run models are selected according to the best validation MRR.

Hyperparameters We conduct an extensive hyperparameter search with the tuple-based and the graph-based models. See Appendix A for details.

6 Results without Additional Features

6.1 Tuple-based

We first investigate how tuple-based models fare when applied to link prediction on VisualSem. Tuple-based models are computationally more efficient than graph-based models, since they model the KB as a set of triplets. We train **TransE** and **DistMult** with OpenKE (Han et al., 2018), and we train **TuckER** following Balazevic et al. (2019).

Table 1 reports each model performance on VisualSem’s test set. We present results when using all negative examples, i.e., using all other nodes in the knowledge graph as corrupted heads or tails given a triplet seen in the graph. We observe that TuckER outperforms both TransE and DistMult, with MRR and Hits@k almost twice as large as the other two algorithms. This is consistent with the finding reported by Balazevic et al. (2019) on

other knowledge graph datasets. Results on the validation set can be found in Appendix B.1.

6.2 Tuple-based vs. Graph-based

Given that TuckER is the best performing tuple-based model, we do not use TransE nor DistMult in further experiments and compare **TuckER** to our graph-based models. We first train vanilla **GAT** and **GraphSage** on link prediction with Deep Graph Library (DGL).⁵ We also experiment with hybrid models where we add a DistMult layer to each graph-based model, thus **GAT+DistMult** and **GraphSage+DistMult**.

We show results in Table 2. We highlight a few points: (1) graph-based baselines GAT and GraphSage perform poorly and are clearly outperformed by TuckER. (2) However, TuckER uses relation features for prediction and is more comparable to hybrid models. Both GAT and GraphSage with a DistMult layer clearly outperform TuckER, which suggests that tuple-based models are worse than graph-based ones on link prediction in VS, and learning relation features is crucial for a good performance. We report results on the validation set in Appendix B.1.

7 Results with Additional Features

Graph-based In this set of experiments, we use our best performing graph-based model architectures and investigate the effect of using additional *textual* and *visual* features for the link prediction task. We incorporate text features computed from the set of multilingual glosses \mathcal{T}_i describing nodes $v_i \in \mathcal{V}$, and image features computed from the set of images \mathcal{I}_i that illustrate v_i . These features are integrated into the model architecture using node and edge gating modules described in Section 4.3.1.

Table 3 shows results for different graph-based representation learning models. We first train and evaluate models using $k = 100$ negative examples. We observe that incorporating both textual and visual features using GraphSage+DistMult yields the best link prediction performance. However, we note that results obtained with GraphSage+DistMult achieves near-perfect scores for Hits@ k for $k > 3$, which suggests that the number of negative examples is too small to observe meaningful differences from the additional features. Therefore, we also train and evaluate models using

⁵<https://www.dgl.ai/>

| | Features | | 100 negative examples | | | | 1000 negative examples | | | |
|-----------|------------------|-----------------|-----------------------|-------------|--------------|--------------|------------------------|-------------|-------------|-------------|
| | \mathcal{T}_i | \mathcal{I}_i | MRR | Hits@1 | Hits@3 | Hits@10 | MRR | Hits@1 | Hits@3 | Hits@10 |
| GAT | \times | \times | 34.8 | 13.6 | 54.4 | 69.3 | 4.4 | 0.0 | 0.0 | 4.7 |
| | \times | \checkmark | 50.2 | 43.3 | 55.6 | 55.6 | <u>29.8</u> | 8.9 | 28.4 | 55.5 |
| | +DistMult | \checkmark | <u>69.4</u> | <u>57.2</u> | <u>81.2</u> | <u>81.2</u> | 24.3 | 7.4 | 26.4 | <u>71.2</u> |
| | \checkmark | \checkmark | 61.8 | 50.4 | 63.8 | 70.1 | 28.2 | <u>9.6</u> | <u>29.3</u> | 69.3 |
| GraphSage | \times | \times | 78.4 | 56.8 | 100.0 | 100.0 | 38.0 | 13.4 | 48.6 | 99.9 |
| | \times | \checkmark | 80.7 | 61.5 | 100.0 | 100.0 | 46.9 | 31.9 | 47.2 | 98.3 |
| | +DistMult | \checkmark | 84.7 | 69.5 | 100.0 | 100.0 | 36.4 | 13.8 | 42.8 | 99.9 |
| | \checkmark | \checkmark | 80.7 | 61.4 | 100.0 | 100.0 | 61.6 | 50.6 | 63.6 | 97.2 |

Table 3: Link prediction results on VisualSem’s test set with additional textual (\mathcal{T}_i) and visual features (\mathcal{I}_i). We show best overall scores per metric in bold, and underline best scores for a model across all features per metric.

$k = 1,000$ negative examples. We find a similar pattern and incorporating both features into GraphSage+DistMult yields the best overall performance. In general, we find that GAT+DistMult underperforms GraphSage+DistMult model. When using both textual and visual features, GraphSage+DistMult’s performance is 33.4% better according to MRR, and 33–40% better according to Hits@ k . We report additional experiments on the validation set in Appendix B.2.

Effects of Multimodal Features The overall impact of additional features is positive. GAT+DistMult always improves with added features, although not consistently according to feature type. GraphSage+DistMult benefits the most when using both textual and visual features from the results with 1000 negative examples.

8 Evaluation on downstream tasks

We use the representations learned with our best-performing models as additional features to ground a multilingual named entity recognition (§8.1) and a visual verb sense disambiguation model (§8.2).

Node Representations We compute node hidden states h_i for all nodes $v_i \in \mathcal{V}$ with our best-performing model, GraphSage+DistMult. We compare four different settings, which use node hidden states trained with: (1) no additional features (**NODE**), (2) gloss features (**TXT**), (3) image features (**IMG**), and (4) both gloss and image features (**TXT+IMG**). We run a forward pass using each setting and generate 100-dimensional node hidden states: h_i^{NODE} , h_i^{TXT} , h_i^{IMG} , $h_i^{\text{TXT+IMG}}$ (Sections 4.2.1 and 4.3). We select the best of the four settings according to validation set performance in each task, and use it to report test set results.

8.1 Named Entity Recognition (NER)

We use two NER datasets: **GermEval 2014** (Benikova et al., 2014), which contains data from German Wikipedia and news corpora, and **WNUT-17** (Derczynski et al., 2017), an English NER dataset which includes user-generated text (e.g., social media, online forums, etc.).

Model We use the pretrained English BERT and the multilingual BERT models for our experiments on WNUT-17 and GermEval, respectively.⁶ For our baseline, we simply fine-tune BERT on the NER data using a multi-layer perceptron (MLP) classifier after the final BERT layer. Let z_i be the final layer representation for an input word x_i . The probabilities of the correct label are:

$$\hat{y}_i = \text{softmax}(\mathbf{W}^n z_i), \quad (9)$$

where \mathbf{W}^n is the classification head. To include additional features from VisualSem, we use VisualSem’s sentence retrieval model to retrieve the top- k closest nodes in the VisualSem graph for each input sentence.

We experiment with two strategies: **i) concat**, where we first concatenate z_i with the representation of the top-1 retrieved node h_i^{RET} and then predict the label as below.

$$\hat{y}_i = \text{softmax}(\mathbf{W}^n [z_i; \mathbf{W}^{\text{RET}} h_i^{\text{RET}}]), \quad (10)$$

and **ii) attend**, where we use an attention mechanism to summarize the top-5 retrieved nodes using z_i as the query, and then concatenate the returned vector to the original hidden state z_i :

$$\hat{y}_i = \text{softmax}(\mathbf{W}^n [z_i; \mathbf{W}^{\text{RET}} \cdot \mathbf{a}]), \quad (11)$$

$$\mathbf{a} = \text{Attention}(z_i, \{h_i^{\text{RET}}\}_{k=1}^5). \quad (12)$$

⁶We use HuggingFace’s (Wolf et al., 2020) models bert-large-cased and bert-base-multilingual-cased available in <https://huggingface.co/>.

| | | Precision | Recall | F1 Score |
|----|--------------------------------------------|-------------|-------------|-------------|
| EN | Baseline | 58.4 | 39.9 | 47.4 |
| | +concat h_i^{IMG} | 57.1 | 39.1 | 46.4 |
| | +attend $\{h_i^{\text{NODE}}\}_{k=1}^5$ | 61.5 | 39.5 | 48.1 |
| DE | Baseline | 86.0 | 86.2 | 86.1 |
| | +concat h_i^{NODE} | 86.2 | 86.6 | 86.4 |
| | +attend $\{h_i^{\text{TXT+IMG}}\}_{k=1}^5$ | 85.7 | 86.0 | 85.9 |

Table 4: NER results on the WNUT-17 (EN) and GermEval (DE) test sets.

Results Table 4 shows our results on test sets. Adding VisualSem entity representations trained with node features yields moderate improvements of 0.7% F1 compared to the baseline for the WNUT-17 (EN) dataset, and 0.3% on the GermEval (DE) dataset. In both cases, the best results are obtained when adding entity representations trained using VisualSem’s graph structure only (i.e., not using any textual or visual information).

8.2 Crosslingual Visual Verb Sense Disambiguation

Crosslingual visual verb sense disambiguation (VSD) is the task of choosing the correct translation given an ambiguous verb in the source language, i.e., a verb with more than one possible translation.

We use **MultiSense** (Gella et al., 2019), a collection of 9,504 images covering 55 English verbs with their unique translations into German and Spanish. Each image is annotated with a translation-ambiguous English verb, a textual description, and the correct translation in the target language.⁷ In our experiments, we use the German verb translations of the dataset, which consists of 154 unique German verbs.

Model We encode the i -th image using the pre-trained ResNet-152 (He et al., 2016) convolutional neural network and use the *pool5* 2048-dimensional activation as the visual features z_i^m . We encode the i -th English verb and its textual description (separated by [SEP] token) using a pre-trained BERT model⁸ and use the final layer English verb token representation as the textual features z_i^t . We do not fine-tune the BERT parameters and only train the task’s classifier head.

To predict the target translation, we concatenate the projected textual and visual features, pass the resulting tensor through a 128-dimensional hidden

⁷github.com/spandanagella/multisense/

⁸We use the bert-large-cased model.

| | Accuracy |
|-----------------------|-------------|
| (Gella et al., 2019) | 55.6 |
| Our Baseline | 94.4 |
| + h_i^{NODE} | 96.8 |
| + h_i^{IMG} | 97.2 |

Table 5: Accuracy on the MultiSense test set (German).

layer followed by a non-linearity. We then apply another projection layer, followed by a softmax.

$$h_i = \text{ReLU}(\mathbf{W}^h[\mathbf{W}^m z_i^m; \mathbf{W}^t z_i^t]), \quad (13)$$

$$\hat{y}_i = \text{softmax}(\mathbf{W}^o h_i). \quad (14)$$

To incorporate information from the knowledge graph, we retrieve the top-1 nearest node representation h_i^{RET} for the i -th input, which is the concatenation of the English verb and the textual description. We then concatenate h_i^{RET} to the input, and instead compute h_i as below.

$$h_i = \text{ReLU}(\mathbf{W}^h[\mathbf{W}^m z_i^m; \mathbf{W}^t z_i^t; h_i^{\text{RET}}]), \quad (15)$$

where the hidden layer size is reduced to 100 such that the number of trained parameters in (13) and (15) is comparable.

Results Table 5 shows our results. Overall, adding VisualSem representations generated with image features yields the best performance compared to the baseline without additional multimodal features. This suggests that crosslingual visual VSD benefits from the additional multimodal information encoded with structural and visual context.

9 Conclusions and Future work

We conducted a systematic comparison of different tuple- and graph-based architectures to learn robust multimodal representations for the VisualSem knowledge graph. We found that additionally using visual and textual information available to nodes in the graph (illustrative images and descriptive glosses, respectively) leads to better node and entity representations, as evaluated on link prediction. Using our best-performing method, a hybrid between a tuple- and graph-based algorithm, we demonstrated the usefulness of our learned entity representations in two downstream tasks: we obtained substantial improvements on crosslingual visual VSD by 2.5% accuracy compared to a strong baseline, and we moderately improved performance for multilingual NER between 0.3%–0.7% F1. In both cases, we used simple downstream architectures

and could likely improve results even further by carefully experimenting with different integration strategies.

We envision many possible avenues for future work. We will incorporate more downstream tasks in our evaluation, including vision-focused tasks (e.g., object detection) and challenging generative tasks (e.g., image captioning). We also plan to apply our framework to other KGs to integrate different types of information, e.g., commonsense knowledge from ConceptNet. Finally, another possibility is to include structured KG representations in large retrieval-based LMs.

Acknowledgments

IC has received funding from the European Union’s Horizon 2020 research and innovation programme under the Marie Skłodowska-Curie grant agreement No 838188. NH is partially supported by the Johns Hopkins Mathematical Institute for Data Science (MINDS) Data Science Fellowship.

CV’s work on this project at New York University was financially supported by Eric and Wendy Schmidt (made by recommendation of the Schmidt Futures program) and Samsung Advanced Institute of Technology (under the project *Next Generation Deep Learning: From Pattern Recognition to AI*) and benefitted from in-kind support by the NYU High-Performance Computing Center. This material is based upon work supported by the National Science Foundation under Grant No. 1922658. Any opinions, findings, and conclusions or recommendations expressed in this material are those of the author(s) and do not necessarily reflect the views of the National Science Foundation.

References

- Houda Alberts, Ningyuan Huang, Yash Deshpande, Yibo Liu, Kyunghyun Cho, Clara Vania, and Iacer Calixto. 2021. [VisualSem: a high-quality knowledge graph for vision and language](#). In *Proceedings of the 1st Workshop on Multilingual Representation Learning*, pages 138–152, Punta Cana, Dominican Republic. Association for Computational Linguistics.
- Mikel Artetxe and Holger Schwenk. 2019. [Massively multilingual sentence embeddings for zero-shot cross-lingual transfer and beyond](#). *Transactions of the Association for Computational Linguistics*, 7:597–610.
- Dzmitry Bahdanau, Kyunghyun Cho, and Yoshua Bengio. 2015. Neural machine translation by jointly learning to align and translate. In *International Conference on Learning Representations (ICLR)*.
- Ivana Balazevic, Carl Allen, and Timothy Hospedales. 2019. [TuckER: Tensor factorization for knowledge graph completion](#). In *Proceedings of the 2019 Conference on Empirical Methods in Natural Language Processing and the 9th International Joint Conference on Natural Language Processing (EMNLP-IJCNLP)*, pages 5185–5194, Hong Kong, China. Association for Computational Linguistics.
- Peter Battaglia, Jessica Blake Chandler Hamrick, Victor Bapst, Alvaro Sanchez, Vinicius Zambaldi, Mateusz Malinowski, Andrea Tacchetti, David Raposo, Adam Santoro, Ryan Faulkner, Caglar Gulcehre, Francis Song, Andy Ballard, Justin Gilmer, George E. Dahl, Ashish Vaswani, Kelsey Allen, Charles Nash, Victoria Jayne Langston, Chris Dyer, Nicolas Heess, Daan Wierstra, Pushmeet Kohli, Matt Botvinick, Oriol Vinyals, Yujia Li, and Razvan Pascanu. 2018. [Relational inductive biases, deep learning, and graph networks](#). *arXiv*.
- Darina Benikova, Chris Biemann, and Marc Reznicek. 2014. [NoSta-D named entity annotation for German: Guidelines and dataset](#). In *Proceedings of the Ninth International Conference on Language Resources and Evaluation (LREC’14)*, pages 2524–2531, Reykjavik, Iceland. European Language Resources Association (ELRA).
- Antoine Bordes, Nicolas Usunier, Alberto Garcia-Duran, Jason Weston, and Oksana Yakhnenko. 2013. [Translating embeddings for modeling multi-relational data](#). In C. J. C. Burges, L. Bottou, M. Welling, Z. Ghahramani, and K. Q. Weinberger, editors, *Advances in Neural Information Processing Systems 26*, pages 2787–2795. Curran Associates, Inc.
- Tom B. Brown, Benjamin Mann, Nick Ryder, Melanie Subbiah, Jared Kaplan, Prafulla Dhariwal, Arvind Neelakantan, Pranav Shyam, Girish Sastry, Amanda Askell, Sandhini Agarwal, Ariel Herbert-Voss, Gretchen Krueger, Tom Henighan, Rewon Child, Aditya Ramesh, Daniel M. Ziegler, Jeffrey Wu, Clemens Winter, Christopher Hesse, Mark Chen, Eric Sigler, Mateusz Litwin, Scott Gray, Benjamin Chess, Jack Clark, Christopher Berner, Sam McCandlish, Alec Radford, Ilya Sutskever, and Dario Amodei. 2020. [Language Models are Few-Shot Learners](#).
- Sreerupa Das, C. Lee Giles, and Guo zheng Sun. 1992. Learning context-free grammars: Capabilities and limitations of a recurrent neural network with an external stack memory. In *CONFERENCE OF THE COGNITIVE SCIENCE SOCIETY*, pages 791–795. Morgan Kaufmann Publishers.
- Leon Derczynski, Eric Nichols, Marieke van Erp, and Nut Limsopatham. 2017. [Results of the WNUT2017 shared task on novel and emerging entity recognition](#). In *Proceedings of the 3rd Workshop on Noisy*

- User-generated Text*, pages 140–147, Copenhagen, Denmark. Association for Computational Linguistics.
- William Fedus, Barret Zoph, and Noam Shazeer. 2021. Switch transformers: Scaling to trillion parameter models with simple and efficient sparsity. *arXiv preprint arXiv:2101.03961*.
- Spandana Gella, Desmond Elliott, and Frank Keller. 2019. Cross-lingual visual verb sense disambiguation.
- Alex Graves, Greg Wayne, and Ivo Danihelka. 2014. *Neural Turing machines*.
- Kelvin Guu, Kenton Lee, Zora Tung, Panupong Pasupat, and Ming-Wei Chang. 2020. Realm: Retrieval-augmented language model pre-training. *arXiv preprint arXiv:2002.08909*.
- Will Hamilton, Zhitao Ying, and Jure Leskovec. 2017. *Inductive representation learning on large graphs*. In I. Guyon, U. V. Luxburg, S. Bengio, H. Wallach, R. Fergus, S. Vishwanathan, and R. Garnett, editors, *Advances in Neural Information Processing Systems 30*, pages 1024–1034. Curran Associates, Inc.
- Xu Han, Shulin Cao, Lv Xin, Yankai Lin, Zhiyuan Liu, Maosong Sun, and Juanzi Li. 2018. Openke: An open toolkit for knowledge embedding. In *Proceedings of EMNLP*.
- Kaiming He, Xiangyu Zhang, Shaoqing Ren, and Jian Sun. 2016. Deep residual learning for image recognition. In *Proceedings of the IEEE Conference on Computer Vision and Pattern Recognition*, pages 770–778.
- Junjie Hu, Sebastian Ruder, Aditya Siddhant, Graham Neubig, Orhan Firat, and Melvin Johnson. 2020. XTREME: A massively multilingual multi-task benchmark for evaluating cross-lingual generalization. *CoRR*, abs/2003.11080.
- Vladimir Karpukhin, Barlas Öguz, Sewon Min, Ledell Wu, Sergey Edunov, Danqi Chen, and Wen-tau Yih. 2020. Dense passage retrieval for open-domain question answering. *arXiv preprint arXiv:2004.04906*.
- Thomas N Kipf and Max Welling. 2016. Semi-supervised classification with graph convolutional networks. *arXiv preprint arXiv:1609.02907*.
- Zhenzhong Lan, Mingda Chen, Sebastian Goodman, Kevin Gimpel, Piyush Sharma, and Radu Soricut. 2020. *Albert: A lite bert for self-supervised learning of language representations*. In *International Conference on Learning Representations*.
- Kenton Lee, Ming-Wei Chang, and Kristina Toutanova. 2019. Latent retrieval for weakly supervised open domain question answering. In *Proceedings of the 57th Annual Meeting of the Association for Computational Linguistics*, pages 6086–6096, Florence, Italy. Association for Computational Linguistics.
- Patrick Lewis, Ethan Perez, Aleksandara Piktus, Fabio Petroni, Vladimir Karpukhin, Naman Goyal, Heinrich Küttler, Mike Lewis, Wen-tau Yih, Tim Rocktäschel, et al. 2020. Retrieval-augmented generation for knowledge-intensive nlp tasks. *arXiv preprint arXiv:2005.11401*.
- Jiasen Lu, Dhruv Batra, Devi Parikh, and Stefan Lee. 2019. *Vilbert: Pretraining task-agnostic visiolinguistic representations for vision-and-language tasks*.
- Tomas Mikolov, Ilya Sutskever, Kai Chen, Greg Corrado, and Jeffrey Dean. 2013. *Distributed representations of words and phrases and their compositionality*.
- Roberto Navigli and Simone Paolo Ponzetto. 2012. Babelnet: The automatic construction, evaluation and application of a wide-coverage multilingual semantic network. *Artificial Intelligence*, 193:217–250.
- Aida Nematzadeh, Sebastian Ruder, and Dani Yogatama. 2020. On memory in human and artificial language processing systems. In *Proceedings of the Bridging AI and Cognitive Science Workshop at ICLR 2020*.
- Fabio Petroni, Patrick Lewis, Aleksandra Piktus, Tim Rocktäschel, Yuxiang Wu, Alexander H. Miller, and Sebastian Riedel. 2020. *How context affects language models’ factual predictions*. In *Automated Knowledge Base Construction*.
- Fabio Petroni, Tim Rocktäschel, Sebastian Riedel, Patrick Lewis, Anton Bakhtin, Yuxiang Wu, and Alexander Miller. 2019. *Language models as knowledge bases?* In *Proceedings of the 2019 Conference on Empirical Methods in Natural Language Processing and the 9th International Joint Conference on Natural Language Processing (EMNLP-IJCNLP)*, pages 2463–2473, Hong Kong, China. Association for Computational Linguistics.
- Alec Radford, Jeffrey Wu, Rewon Child, David Luan, Dario Amodei, and Ilya Sutskever. 2019. Language models are unsupervised multitask learners. *OpenAI blog*, 1(8):9.
- Olga Russakovsky, Jia Deng, Hao Su, Jonathan Krause, Sanjeev Satheesh, Sean Ma, Zhiheng Huang, Andrej Karpathy, Aditya Khosla, Michael Bernstein, Alexander C. Berg, and Li Fei-Fei. 2015. *Imagenet large scale visual recognition challenge*. *Int. J. Comput. Vision*, 115(3):211–252.
- Victor Sanh, Lysandre Debut, Julien Chaumond, and Thomas Wolf. 2019. *Distilbert, a distilled version of bert: smaller, faster, cheaper and lighter*. In *5th Workshop on Energy Efficient Machine Learning and Cognitive Computing - NeurIPS 2019*.
- Michael Schlichtkrull, Thomas N. Kipf, Peter Bloem, Rianne van den Berg, Ivan Titov, and Max Welling. 2017. *Modeling relational data with graph convolutional networks*.

- Emma Strubell, Ananya Ganesh, and Andrew McCallum. 2019. [Energy and policy considerations for deep learning in NLP](#). In *Proceedings of the 57th Annual Meeting of the Association for Computational Linguistics*, pages 3645–3650, Florence, Italy. Association for Computational Linguistics.
- Zhou Su, Chen Zhu, Yinpeng Dong, Dongqi Cai, Yurong Chen, and Jianguo Li. 2018. Learning visual knowledge memory networks for visual question answering. In *Proceedings of the IEEE Conference on Computer Vision and Pattern Recognition*, pages 7736–7745.
- Sainbayar Sukhbaatar, Jason Weston, Rob Fergus, et al. 2015. End-to-end memory networks. In *Advances in neural information processing systems*, pages 2440–2448.
- Hao Tan and Mohit Bansal. 2019. [Lxmert: Learning cross-modality encoder representations from transformers](#).
- Ledyard Tucker. 1966. [Some mathematical notes on three-mode factor analysis](#). *Psychometrika*, 31(3):279–311.
- Petar Veličković, Guillem Cucurull, Arantxa Casanova, Adriana Romero, Pietro Liò, and Yoshua Bengio. 2018. [Graph attention networks](#). In *International Conference on Learning Representations*.
- Alex Wang, Yada Pruksachatkun, Nikita Nangia, Amanpreet Singh, Julian Michael, Felix Hill, Omer Levy, and Samuel Bowman. 2019a. [Superglue: A stickier benchmark for general-purpose language understanding systems](#). In H. Wallach, H. Larochelle, A. Beygelzimer, F. d’Alché Buc, E. Fox, and R. Garnett, editors, *Advances in Neural Information Processing Systems 32*, pages 3266–3280. Curran Associates, Inc.
- Alex Wang, Amanpreet Singh, Julian Michael, Felix Hill, Omer Levy, and Samuel R. Bowman. 2019b. [GLUE: A multi-task benchmark and analysis platform for natural language understanding](#). In *International Conference on Learning Representations*.
- Junbo Wang, Wei Wang, Yan Huang, Liang Wang, and Tieniu Tan. 2018. M3: Multimodal memory modelling for video captioning. In *Proceedings of the IEEE Conference on Computer Vision and Pattern Recognition*, pages 7512–7520.
- Jason Weston, Sumit Chopra, and Antoine Bordes. 2014. Memory networks. *arXiv preprint arXiv:1410.3916*.
- Thomas Wolf, Lysandre Debut, Victor Sanh, Julien Chaumond, Clement Delangue, Anthony Moi, Pierric Cistac, Tim Rault, Rémi Louf, Morgan Funtowicz, Joe Davison, Sam Shleifer, Patrick von Platen, Clara Ma, Yacine Jernite, Julien Plu, Canwen Xu, Teven Le Scao, Sylvain Gugger, Mariama Drame, Quentin Lhoest, and Alexander M. Rush. 2020. [Huggingface’s transformers: State-of-the-art natural language processing](#).
- Caiming Xiong, Stephen Merity, and Richard Socher. 2016. Dynamic memory networks for visual and textual question answering. In *International conference on machine learning*, pages 2397–2406.
- Bishan Yang, Wen-tau Yih, Xiaodong He, Jianfeng Gao, and Li Deng. 2015. [Embedding entities and relations for learning and inference in knowledge bases](#). In *3rd International Conference on Learning Representations, ICLR 2015, San Diego, CA, USA, May 7-9, 2015, Conference Track Proceedings*.
- Fei Yu, Jiji Tang, Weichong Yin, Yu Sun, Hao Tian, Hua Wu, and Haifeng Wang. 2021. [Ernie-vil: Knowledge enhanced vision-language representations through scene graph](#).
- Zheng Zeng, R. M. Goodman, and P. Smyth. 1994. Discrete recurrent neural networks for grammatical inference. *IEEE Transactions on Neural Networks*, 5(2):320–330.

A Hyperparameters

TransE We perform a grid search over the learning rate $\alpha \in \{0.01, 0.1, 1\}$, embedding dimension $d \in \{100, 200, 300, 400\}$, and margin $m \in \{1, 5, 10\}$. The optimal configuration is $\alpha = 1$, $d = 200$, and $m = 5$. In training, the number of negative examples is fixed to 25.

DistMult We perform a grid search over the learning rate $\alpha \in \{0.1, 0.01, 0.001\}$, embedding dimension $\in \{100, 200\}$, and weight decay rate $\lambda \in \{0.01, 0.0001\}$. The optimal configuration is $\alpha = 0.1$, $d = 100$, and $\lambda = 0.0001$.

TuckER We conduct a grid search over the learning rate $\alpha \in \{0.01, 0.005, 0.003, 0.001, 0.0005\}$ and weight decay rate $\lambda \in \{1, 0.995, 0.99\}$. Entity and relation embedding dimensions are fixed at 200 and 30 respectively. The optimal configuration is $\alpha = 0.03$, $\lambda = 1$, input dropout = 0.2, dropout = 0.2, and label smoothing rate = 0.1.

GraphSage and GraphSage+DistMult Both models are trained for a maximum of 100 epochs and we early stop if validation MRR does not improve for over 20 epochs. We search for learning rate $\{0.001, 0.002\}$ and weight decay $\{0, 0.0001, 0.00005, 0.00001\}$. We use 100-dimensional node and relation embeddings, and two graph layers (Equation 2) with a dropout rate of 0.5 applied to the input of each layer. Both models have batch size 10^4 for 100 negative examples and 10^3 for 1000 negative examples.

GAT and GAT+DistMult Both models are trained for a maximum of 100 epochs, and we also early stop if validation MRR does not improve for over 20 epochs. We perform a grid search over the learning rate $\alpha \in \{0.1, 0.001, 0.0001\}$, the embedding dimension $d \in \{100, 200\}$, number of attention heads $n_h \in \{2, 4\}$, and weight decay rate $\lambda \in \{0, 0.001, 0.005, 0.0001\}$. The optimal configuration is $\alpha = 0.001$, $d = 100$, $n_h = 2$, and $\lambda = 0.005$. Both models have batch size 10^4 for 100 negative examples and 10^3 for 1000 negative examples.

B Link Prediction Results

B.1 Without Additional Features

In Tables 6 and 7 we show additional results on VisualSem link prediction on the validation set, obtained with tuple-based, graph-based, and hybrid

| | MRR | Hits@1 | Hits@3 | Hits@10 |
|----------|------------|------------|------------|-------------|
| TransE | 3.5 | 0.3 | 3.7 | 9.3 |
| DistMult | 3.7 | 1.9 | 3.6 | 7.7 |
| Tucker | 6.2 | 3.5 | 6.2 | 11.3 |

Table 6: Link prediction results on VisualSem’s validation set using all negative samples.

| | R | MRR | Hits@1 | Hits@3 | Hits@10 |
|-----------|---|-------------|-------------|--------------|--------------|
| TuckER | ✓ | 58.7 | 47.5 | 64.4 | 80.3 |
| GAT | ✗ | 10.0 | 4.0 | 12.7 | 29.8 |
| +DistMult | ✓ | 75.0 | 61.2 | 88.6 | 88.6 |
| GraphSage | ✗ | 8.7 | 2.4 | 6.5 | 18.1 |
| +DistMult | ✓ | 74.9 | 49.8 | 100.0 | 100.0 |

Table 7: Link prediction results on VisualSem’s validation set using 100 negative samples. **R**: denotes whether the model learn relation features or not.

models. We note that results are similar to the ones obtained on the test set and reported in Tables 1 and 2.

B.2 Additional Features

We report link prediction results on VisualSem’s validation set when models have access to additional features (i.e., gloss and/or image features) in Table 8.

C Node and Edge Gating

C.1 Node Gating

We gate features $\{t_i, m_i\}$ directly with node embeddings v_i , and denote the node gating function f_n with parameters θ_n to transform node embeddings and additional features and compute *informed* node embeddings.

Text When integrating only textual features into node embeddings v_i , we compute $v_i^t = f_n(v_i, t_i)$ as below.

$$\begin{aligned} s_g^t &= \text{MLP}_g^t([v_i; \mathbf{W}_g^t \cdot t_i]), \\ v_i^t &= s_g^t \cdot t_i + (1 - s_g^t) \cdot v_i, \end{aligned} \quad (16)$$

where \mathbf{W}_g^t is a trained projection matrix for gloss features, s_g^t is a gating scalar computed using a multi-layer perceptron MLP_g^t , and v_i^t are node embeddings informed by glosses \mathcal{T}_i .

Image When integrating only image features into node embeddings v_i , we compute $v_i^m = f_n(v_i, m_i)$ as below.

$$\begin{aligned} s_g^m &= \text{MLP}_g^m([v_i; \mathbf{W}_g^m \cdot m_i]), \\ v_i^m &= s_g^m \cdot m_i + (1 - s_g^m) \cdot v_i, \end{aligned} \quad (17)$$

| | Features | | 100 negative examples | | | | 1000 negative examples | | | |
|-----------|------------------|-----------------|-----------------------|-------------|--------------|--------------|------------------------|-------------|-------------|-------------|
| | \mathcal{T}_i | \mathcal{I}_i | MRR | Hits@1 | Hits@3 | Hits@10 | MRR | Hits@1 | Hits@3 | Hits@10 |
| GAT | \times | \times | 75.0 | 61.2 | 88.6 | 88.6 | <u>34.2</u> | <u>14.6</u> | 41.0 | <u>87.9</u> |
| | \times | \checkmark | <u>79.6</u> | <u>66.6</u> | <u>92.5</u> | <u>92.5</u> | 30.8 | 11.8 | 36.6 | 83.4 |
| | +DistMult | \checkmark | 71.4 | 59.0 | 83.6 | 83.6 | 28.2 | 9.1 | 32.9 | 83.4 |
| | \checkmark | \checkmark | 70.9 | 57.9 | 83.6 | 83.6 | 30.5 | 11.7 | 35.0 | 83.4 |
| GraphSage | \times | \times | 74.9 | 49.8 | 100.0 | 100.0 | 39.6 | 19.0 | 43.7 | 99.9 |
| | \times | \checkmark | 83.5 | 67.1 | 100.0 | 100.0 | 42.4 | 25.2 | 44.1 | 98.7 |
| | +DistMult | \checkmark | 84.0 | 68.0 | 100.0 | 100.0 | 35.2 | 11.6 | 41.8 | 99.8 |
| | \checkmark | \checkmark | 84.5 | 68.9 | 100.0 | 100.0 | 59.3 | 49.3 | 58.8 | 94.4 |

Table 8: Link prediction results on VisualSem’s validation set with additional features. We show best overall scores per metric in bold, and we underline best scores for a single model across all features per metric.

where similarly \mathbf{W}_g^m is a trained projection matrix for image features, s_g^m is a gating scalar computed with MLP_g^m , and \mathbf{v}_i^m are node embeddings informed by images \mathcal{I}_i .

Text+Image Finally, when integrating both textual and image features into \mathbf{v}_i , informed node embeddings $\mathbf{v}_i^{t,m} = f_n(\mathbf{v}_i, \mathbf{t}_i, \mathbf{m}_i)$ are computed below.

$$\mathbf{v}_i^{t,m} = \mathbf{W}_g^{t,m} \cdot [\mathbf{v}_i^t; \mathbf{v}_i^m] \quad (18)$$

where $\mathbf{W}_g^{t,m}$ is a projection matrix and $\mathbf{v}_i^{t,m}$ are node embeddings informed by both glosses and images.

C.2 Edge (Relation) Gating

Given a triplet (v_i, e_r, v_j) , we gate text features \mathbf{t}_i with edge embeddings \mathbf{e}_r as below.

$$\begin{aligned} \mathbf{t}_r &= \frac{\mathbf{W}_d^t \mathbf{t}_i + \mathbf{W}_d^t \mathbf{t}_j}{2}, \\ s_d^t &= \text{MLP}_d^t([\mathbf{e}_r; \mathbf{t}_r]), \\ \mathbf{e}_r^t &= s_d^t \cdot \mathbf{t}_r + (1 - s_d^t) \cdot \mathbf{e}_r, \end{aligned} \quad (19)$$

where \mathbf{W}_d^t is a trained projection matrix, \mathbf{t}_r are average gloss features for nodes v_i and v_j , \mathbf{e}_r^t are edge embeddings informed by glosses $\mathcal{T}_i \cup \mathcal{T}_j$, and s_d^t is a gating scalar computed using a multi-layer perceptron MLP_d^t . Similarly, we gate image features \mathbf{m}_i with edge embeddings \mathbf{e}_r as below.

$$\begin{aligned} \mathbf{m}_r &= \frac{\mathbf{W}_d^m \mathbf{m}_i + \mathbf{W}_d^m \mathbf{m}_j}{2}, \\ s_d^m &= \text{MLP}_d^m([\mathbf{e}_r; \mathbf{m}_r]), \\ \mathbf{e}_r^m &= s_d^m \cdot \mathbf{m}_r + (1 - s_d^m) \cdot \mathbf{e}_r, \end{aligned} \quad (20)$$

where \mathbf{W}_d^m is a trained projection matrix, \mathbf{m}_r are average image features for nodes v_i and v_j , \mathbf{e}_r^m are edge embeddings informed by images $\mathcal{I}_i \cup \mathcal{I}_j$, and

s_d^m is a gating scalar computed using a multi-layer perceptron MLP_d^m . Finally, we combine both text and image features as described in Equation 21.

$$\mathbf{e}_r^{t,m} = \mathbf{W}_d^{t,m} [\mathbf{e}_r^t; \mathbf{e}_r^m] \quad (21)$$

where $\mathbf{W}_d^{t,m}$ is a parameter matrix and $\mathbf{e}_{i,j}^r$ are edge embeddings informed by glosses and images.

C.3 Training

To train hybrid models GAT+DistMult and GraphSage+DistMult with additional features, we use (1) only gloss features \mathcal{T}_i , i.e. node and edge embeddings computed by Equations 16 and 19, respectively; (2) only image features \mathcal{I}_i , i.e. node and edge embeddings computed by Equations 17 and 20, respectively; (3) both gloss and image features $\mathcal{T}_i, \mathcal{I}_i$, i.e. node and edge embeddings computed by Equations 18 and 21, respectively.

D Downstream Tasks

D.1 NER Hyperparameters

We use a BERT base architecture for the German NER model (GermEval) and a BERT large architecture for the English NER model (WNUT-17), in both cases using case-sensitive models. For both GermEval and WNUT-17, the best performing model configuration uses a projection of the original VisualSem graph representations (100-dimensional) into the respective BERT encoder dimensions (mBERT 768-dimensional, English monolingual BERT 1024-dimensional). These projected features are concatenated with the corresponding BERT encoding, which is then used as input to the prediction head.

D.2 NER Ablation

We report additional NER experiment results on the WNUT-17 and GermEval validation sets us-

| | | Precision | Recall | F1 Score |
|----|-------------------------|-------------|-------------|-------------|
| EN | Baseline | 70.1 | 50.7 | 58.8 |
| | $+h_i^{\text{NODE}}$ | 68.7 | 53.1 | 59.9 |
| | $+h_i^{\text{IMG}}$ | 68.5 | 54.4 | 60.7 |
| | $+h_i^{\text{TXT}}$ | 65.8 | 54.4 | 59.6 |
| | $+h_i^{\text{TXT+IMG}}$ | 64.2 | 53.0 | 58.1 |
| DE | Baseline | 84.7 | 87.8 | 86.2 |
| | $+h_i^{\text{NODE}}$ | 85.2 | 88.5 | 86.8 |
| | $+h_i^{\text{IMG}}$ | 84.8 | 88.1 | 86.4 |
| | $+h_i^{\text{TXT}}$ | 85.0 | 88.1 | 86.5 |
| | $+h_i^{\text{TXT+IMG}}$ | 85.0 | 88.3 | 86.6 |

Table 9: Concatenation with $100 \times d \in \{1024, 768\}$ projection matrix

| | Precision | Recall | F1 Score |
|-------------------------|-------------|-------------|-------------|
| Baseline | 70.1 | 50.7 | 58.5 |
| $+h_i^{\text{NODE}}$ | 66.3 | 50.7 | 57.5 |
| $+h_i^{\text{IMG}}$ | 58.6 | 51.3 | 54.7 |
| $+h_i^{\text{TXT}}$ | 68.0 | 53.5 | 59.9 |
| $+h_i^{\text{TXT+IMG}}$ | 65.7 | 52.5 | 58.4 |

Table 10: Gating with 100×1024 projection matrix

| | Precision | Recall | F1 Score |
|-------------------------|-------------|-------------|-------------|
| Baseline | 70.1 | 50.7 | 58.5 |
| $+h_i^{\text{NODE}}$ | 65.5 | 53.2 | 58.7 |
| $+h_i^{\text{IMG}}$ | 68.6 | 51.6 | 58.9 |
| $+h_i^{\text{TXT}}$ | 67.3 | 50.0 | 57.4 |
| $+h_i^{\text{TXT+IMG}}$ | 67.9 | 51.2 | 58.4 |

Table 11: Gating with 100×100 projection matrix

| | Precision | Recall | F1 Score |
|-------------------------|-------------|-------------|-------------|
| Baseline | 70.1 | 50.7 | 58.5 |
| $+h_i^{\text{NODE}}$ | 54.7 | 45.9 | 49.9 |
| $+h_i^{\text{IMG}}$ | 66.3 | 52.8 | 58.8 |
| $+h_i^{\text{TXT}}$ | 65.9 | 53.0 | 58.8 |
| $+h_i^{\text{TXT+IMG}}$ | 67.8 | 51.3 | 58.4 |

Table 12: Concatenation with 100×100 projection matrix

ing (1) concatenation with $100 \times d \in \{1024, 768\}$ projection matrix (Table 9), and on the WNUT-17 validation set using gating with 100×1024 projection matrix (Table 10), gating with 100×100 projection matrix (Table 11), concatenation with 100×100 projection matrix (Table 12), gating without projection plus fine-tuning node hidden states (Table 13), and concatenation without projection plus fine-tuning node hidden states (Table 14).

| | Precision | Recall | F1 Score |
|-------------------------|-------------|-------------|-------------|
| Baseline | 70.1 | 50.7 | 58.5 |
| $+h_i^{\text{NODE}}$ | 70.7 | 51.7 | 59.7 |
| $+h_i^{\text{IMG}}$ | 67.1 | 50.8 | 57.9 |
| $+h_i^{\text{TXT}}$ | 69.8 | 52.9 | 60.2 |
| $+h_i^{\text{TXT+IMG}}$ | 55.2 | 48.1 | 51.4 |

Table 13: Gating without projection plus fine-tuning node hidden states

| | Precision | Recall | F1 Score |
|-------------------------|-------------|-------------|-------------|
| Baseline | 70.1 | 50.7 | 58.5 |
| $+h_i^{\text{NODE}}$ | 67.7 | 51.2 | 58.3 |
| $+h_i^{\text{IMG}}$ | 64.6 | 49.8 | 56.2 |
| $+h_i^{\text{TXT}}$ | 65.5 | 52.3 | 58.2 |
| $+h_i^{\text{TXT+IMG}}$ | 67.4 | 52.0 | 58.7 |

Table 14: Concatenation without projection plus fine-tuning node hidden states

| Our Baseline | $+h_i^{\text{NODE}}$ | $+h_i^{\text{TXT}}$ | $+h_i^{\text{TXT+IMG}}$ | $+h_i^{\text{IMG}}$ |
|---------------------|----------------------|---------------------|-------------------------|---------------------|
| 95.7 | 96.1 | 97.8 | 96.4 | 95.5 |

Table 15: Accuracy on the German MultiSense validation set.

D.3 Visual Verb Sense Disambiguation Ablation

For the German portion of the datasets, there are 707 tuples in the form *English verb*, *English query*, *German verb*. We divided the dataset into 75% training, 10% validation and 15% test splits, and used minibatch size 16, following the set up in Gella et al. (2019). We use learning rate 0.0005 and dropout with probability 0.1 across all settings.

Table 15 reports validation set results on MultiSense using different graph representations.